Bioorganic & Medicinal Chemistry 23 (2015) 429–438

Contents lists available at ScienceDirect

Bioorganic & Medicinal Chemistry

journal homepage: www.elsevier.com/locate/bmc

Design and synthesis of a novel series of histamine H_3 receptor antagonists through a scaffold hopping strategy

Zhongli Gao [a,*], William J. Hurst [b,†], Daniel Hall [b], Ryan Hartung [b,‡], William Reynolds [b], Jiesheng Kang [c], Raisa Nagorny [b], James A. Hendrix [b,§], Pascal G. George [d]

[a] LGCR SMRPD Chemical Research, Sanofi US, 153-1-130, 153 2nd Ave, Waltham, MA 02451, USA
[b] Sanofi US, 55C-420A, 55 Corporate Drive, Bridgewater, NJ 08807, USA
[c] Proteogenomics, Sanofi/Genzyme R&D Center, 49 New York Avenue, Framingham, MA 01701, USA
[d] Sanofi R&D, 1, Avenue Pierre Brossolette, Chilly-Mazarin 91385, France

ARTICLE INFO

Article history:
Received 25 September 2014
Revised 8 December 2014
Accepted 16 December 2014
Available online 23 December 2014

Keywords:
Histamine H_3 receptor antagonist/inverse agonist
Structure activity relationship
Scaffold hopping
Cardiac myocyte model

ABSTRACT

Lead compounds 5-fluoro-2-methyl-*N*-[2-methyl-4-(2-methyl-[1,3′]bipyrrolidinyl-1′-yl)-phenyl]-benzamide (**1**), tetrahydro-pyran-4-carboxylic acid [((2*S*,3′*S*)-2-methyl-[1,3′]bipyrrolidinyl-1′-yl)-phenyl]-amide (**2**), and 3,5-dimethyl-isoxazole-4-carboxylic acid [((2*S*,3′*S*)-2-methyl-[1,3′]bipyrrolidinyl-1′-yl)-phenyl]-amide (**3**) discovered in our laboratory, displayed high histamine H_3 receptor (H_3R) affinity, good selectivity and weak human Ether-à-go-go-Related Gene (hERG) channel affinity with desirable overall physico-chemical and pharmacokinetic (PK) profiles. Herein, we describe the design and synthesis of a novel series of H_3R antagonists utilizing a scaffold hopping strategy. Further structure–activity relationship (SAR) studies of the series culminated in the identification of ((2*S*,3′*S*)-2-methyl-[1,3′]bipyrrolidinyl-1′-yl)-naphthalene-2-carboxylic acid (tetrahydro-pyran-4-yl)-amide (**4c**) and -[4-((2*S*,3′*S*)-2-methyl-[1,3′]bipyrrolidinyl-1′-yl)-phenyl]-*N*-(tetrahydro-pyran-4-yl)-acetamide (**4d**), which exhibited good H_3R affinity in vitro, good selectivity, and desirable PK properties. Compounds **4c** and **4d** were also assessed in cardiac safety experiments. In particular, the effects of the compounds on action potentials recorded from ventricular myocytes isolated from guinea pigs were used to screen compounds that not only displayed a low affinity towards hERG channel, but also had lower interference with other cardiac ion channels. Compound **4c** did not alter the major parameters in this model system at $\leqslant 10$ μM, and no significant induction of any major haemodynamic effect when intravenously administered at 3 mg/kg dose to anaesthetized mongrel dogs. Compound **4c** is a new promising lead as orally potent and selective H_3R antagonist belonging to a distinct structural class.

1. Introduction

Since the discovery of the histamine H_3 receptor (H_3R),[1] a G-protein coupled receptor, a wide variety of its functions for health and disease have been elucidated.[2–7] The receptor is localized predominantly in the central and peripheral nervous systems. When activated, the H_3R can suppress the release of neurotransmitters that include not only histamine but also dopamine, acetylcholine, norepinephrine, serotonin, glutamate and others (negative modulation).[8,9] A key aspect of the unresolved puzzle of H_3R pharmacology is that, in addition to possible roles in cognition[6] such as Alzheimer's disease, as well as sleep disorders, H_3R ligands have therapeutic potential in diseases and disorders such as attention deficit hyperactivity disorder,[10–13] schizophrenia,[14] obesity,[15,16] epilepsy,[17] neuropathic pain,[18] myocardial dysfunction[19] and others. This diversity of indications is difficult to rationalize with current ideas regarding uniform ligand–receptor–G-protein interactions. However, increasing evidence[2,12] supports the complexity of the CNS histamine system, including histamine-containing neurons, H_3R, interactions with signal transduction pathways and the diversity of neurotransmitters whose syntheses and/or release are modulated by H_3R. Taken together, these and other findings suggest the potential utility of H_3R antagonists for the treatment of central nervous system (CNS) diseases. Much effort has focused

* Corresponding author. Tel.: +1 781 434 3635.
E-mail addresses: zhongli.gao@sanofi.com (Z. Gao), william.hurst@sanofi.com (W.J. Hurst), jhendrix@alz.org (J.A. Hendrix).
† Tel.: +1 908 981 3723.
‡ Current address: Combinatorial Chemistry 1, Sanofi US, 2090 East Innovation Park Drive, Oro Valley, AZ 8575, USA.
§ Present address: Alzheimer's Association, 225 N. Michigan Ave., 17th Floor, Chicago, IL 60601, USA. Tel.: +1 212 568 0365.

http://dx.doi.org/10.1016/j.bmc.2014.12.036
0968-0896/

on understanding H_3R physiology and the discovery of increasingly selective and potent H_3R ligands with therapeutic potential.[7,20,21] A few H_3R antagonists have entered into clinical development (for review, see Refs. 7,20–22). However, no H_3R antagonist compound is approved for clinical use. There is still an unmet need to discover novel, structurally diverse and highly selective H_3R antagonists with characterized therapeutic utility.

Earlier work from our group[23–26] revealed a series of H_3R antagonists/inverse agonists that displayed diverse pharmacological profiles (Fig. 1): compound **1** exhibited oral activity in ob./ob. mouse food intake inhibition model; compound **2** demonstrated oral awakening effect in rat; compound **3** showed oral activity in rat forced swim test (FST). Following these successes, the focus of our H_3R program was shifted towards the discovery of a *structurally diverse* novel series. The new lead compound in the novel series have to be comparable with the leads **1**–**3** in certain aspects, such as high H_3R affinity, good selectivity, acceptable human Ether-à-go-go-Related Gene (hERG) channel selectivity and desirable overall physico-chemical, as well as pharmacokinetic (PK) profiles but belong to a distinct and novel structural class.

Previous structure activity relationship studies[24,25,27] revealed that the bipyrrolidine moiety with 2*S*,3′*S* stereochemistry was preferred. It would be optimal to keep the bipyrrolidine moiety unchanged for the present objective. The novel series could be derived through a scaffold hopping strategy, for example, by using an 'inverse amide' to link the left-handed heterocyclic moiety (designated as '*HC*' in Fig. 2, structure **4**) to the 'Central core' as indicated in structure **4**. The *HC* moiety and the central core can be optimized simultaneously (Fig. 2). The rationale for such a design was stemmed from the understanding of the previous SAR studies and our pharmacophore hypothesis. The H_3R ligands should consistent of three components: the right-handed basic center which are essential for H_3R activity; the right-handed heterocyclic (designated as '*HC*') which are substantially enhancing H_3R activity; the Central core with proper lipophilicity and a linker which provides the scaffold to hold the right-handed and the left-handed moieties together in preferred angle and distance so that H_3R recognition and binding could be optimal. The design, synthesis, and the pharmacological assessment of this novel series of H_3R ligands are thus described herein.

2. Results and discussion

Compounds **4a**–**4e** (Table 1) were synthesized as highlighted in Scheme 1. The synthesis began with the commercially available amine **5**, which was coupled with the substituted aryl carboxylic acid **6** to obtain amide **7**. Intermediate **7** was then condensed with (2*S*,3′*S*)-2-methyl-[1,3′]bipyrrolidinyl (**8**) (for synthesis, see Ref. 27) by using the reaction conditions adapted from the Buchwald protocol[28,29] to yield the desired amide analogs **4a**–**4e**.

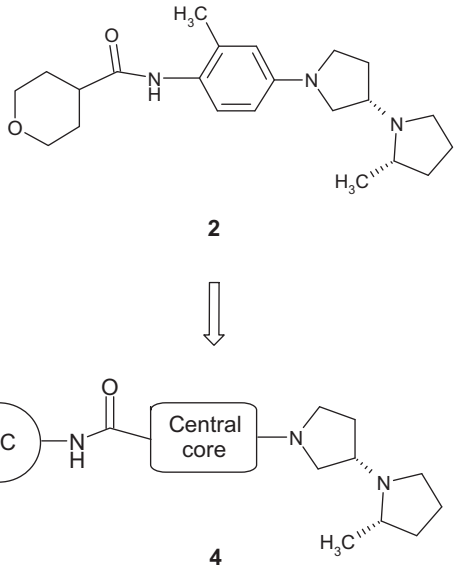

Figure 2. Design strategy for deriving a novel series of H_3R ligands.

Compound **4e** was further derivatized to **4f**–**4h** following the synthetic route illustrated in Scheme 2.

Thus, the *t*-butyl carbamate in compound **4e** was removed under acidic conditions to give compound **4f**. The secondary amine **4f** was converted into tertiary amine **4g** by standard reductive amination with cyclopentane-carboxaldehyde.

Compound **4i** was synthesized in a different route, as shown in Scheme 3. *para*-Bromo-benzoic acid *t*-butyl ester **9** was condensed with **8** to obtain (2*S*,3′*S*)-2-methyl-[1,3′]bipyrrolidinyl-benzoic acid *t*-butyl ester **10**. The *t*-butyl protection group was then removed by acidic hydrolysis (HCl in dioxane) to yield acid **11**, which was subsequently coupled with various amines **5** to obtain the desired amide analog **4i** (Table 1).

Compound **4j** was synthesized similarly, as shown in Scheme 4. 4-Bromo-benzaldehy was condensed with piperidine-4-carboxylic acid methyl ester to benzylamine **12**. Simple ester–amide exchange reaction with gave rise to amide **13**. Finally, condensation with **8** yielded the desired compound **4j**.

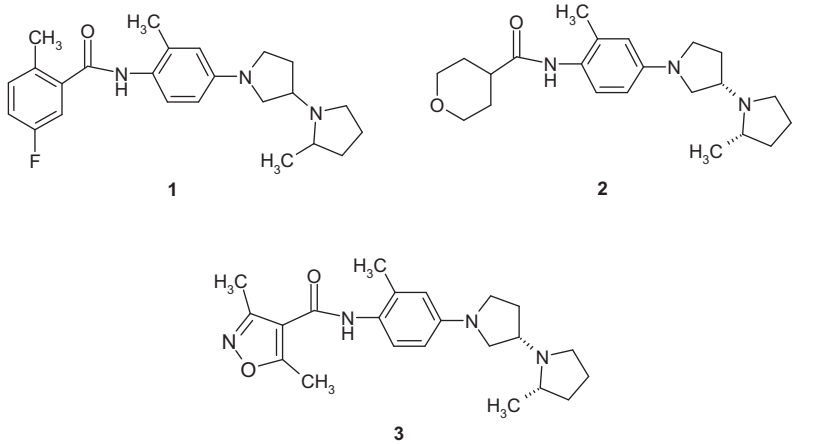

Figure 1. Structures of H_3R antagonists.

Table 1
Histamine-3 receptor H_3R affinity and calculated physico-chemical properties

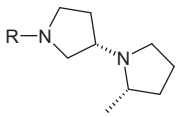

4a-4j

No.	R	H_3R binding			*c*log*P*	*c*log$D_{7.4}$	MW	PSA
		Rhesus K_i (nM)	Rat K_i (nM)	Mouse K_i (nM)				(Å^2)
2	–	0.8	1.0	10.0	2.2	−0.2	371.52	45
4a	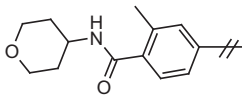	1.5 ± 0.3	19.7 ± 5.8	12.1 ± 5.3	1.7	−0.7	371.52	45
4b	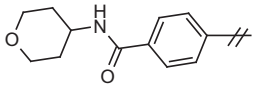	2.0 ± 0.1	15.0 ± 10.3	10.1 ± 13.7	1.5	−0.9	357.49	45
4c	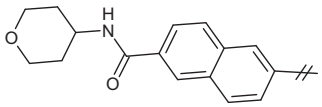	3.0 ± 0.5	9.8 ± 1.2	19.6 ± 4.0	2.2	−0.3	407.55	45
4d	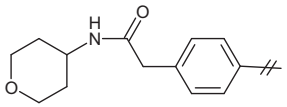	2.5 ± 0.1	8.3 ± 2.8	10.8 ± 1.0	2.5	0.1	371.52	45
4e	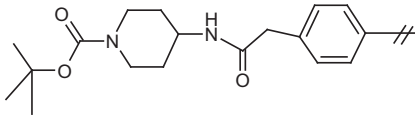	2.8 ± 0.1	19.4 ± 0.1		3.4	0.9	470.65	65
4f	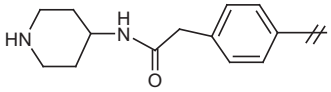	0.8 ± 0.2	1.1 ± 0.1		1.9	−2.1	370.53	48
4g	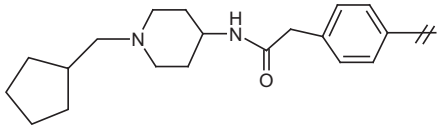	0.7 ± 0.5	1.3 ± 0.1		4.2	0.4	452.68	39
4h	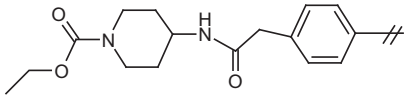	1.6 ± 0.1	8.3 ± 0.1		2.6	0.2	442.59	65
4i	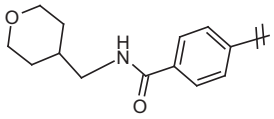	1.2 ± 0.8	19.1 ± 7.1	40.3 ± 18.8	2.1	−0.3	371.52	45
4j	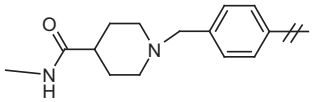	0.47	0.93	4.4	2.2	−1.1	384.56	39

Analogs **4a**–**4j** were then tested in H_3R binding assays. A correlation between human and rhesus H_3R binding affinity (see Ref. 24,25) seemed apparent. The project team took advantage of this observation by using rhesus monkey H_3R binding data as the first tier screening for all the synthesized compounds. The choice of rhesus monkey, rat, and mouse H_3R binding assay as the first tier screening, instead of human H_3R binding assay in parallel, was mainly due to the limited resources and aggressive timelines. Furthermore, the rhesus monkey data would be useful for pharmacological assessment of the selected compounds in acute in vivo models. Therefore, all the compounds synthesized were evaluated in H_3R binding assays by displacement of [^{3}H]*N*-α-methylhistamine in membranes isolated from a CHO cell line stably transfected with the rhesus monkey H_3 receptors (rh-H_3R), rat (r-H_3R) and mouse (m-H_3R). The results are listed in Table 1. The calculated physicochemical properties (*c*log*P*, *c*log$D_{7.4}$, PSA) (calculated using ACD/Labs methods) were used as a guide to select the optimal substituents for the '*HC*' and the 'Central core'. The in vitro ADME data are given in Table 2. The metabolic stability was determined with an in vitro assay using S9 fractions of human, mouse, and rat liver microsomes. Values are expressed as a percent of parent compound metabolized after 15 min incubation at 37 °C. The hERG affinity was performed using a patch-clamp technique in the whole-cell configuration on Chinese hamster ovary (CHO) cells. The inhibition of

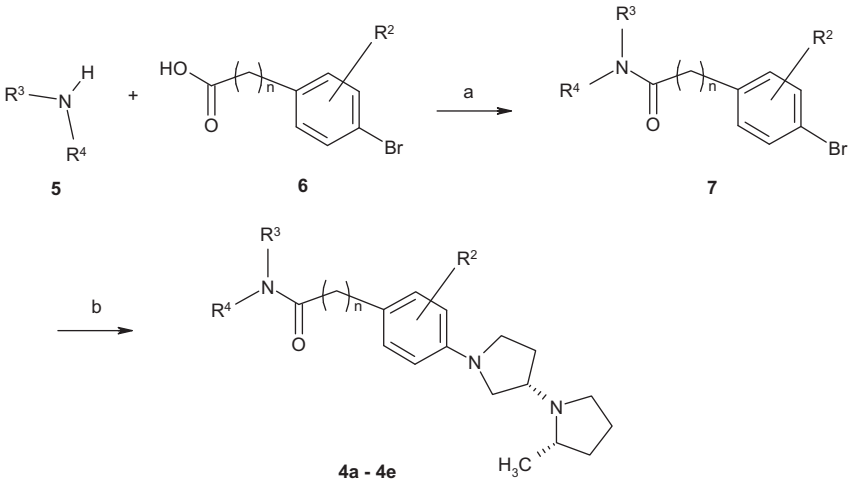

Scheme 1. Syntheses of analogs **4a**–**4e**. Reagents and conditions: (a) *N*-methylmorpholine, HOBT, EDC·HCl, CH_2Cl_2, DMF, rt, 16 h, 100% yield; (b) sodium *tert*-butoxide, tris(dibenzylideneacetone)-dipalladium-(0), BINAP, toluene, (2*S*,3′*S*)-2-methyl-[1,3′]bipyrrolidinyl dihydrochloride (**8**), 85 °C (external), 15 h, 70–72% yield.

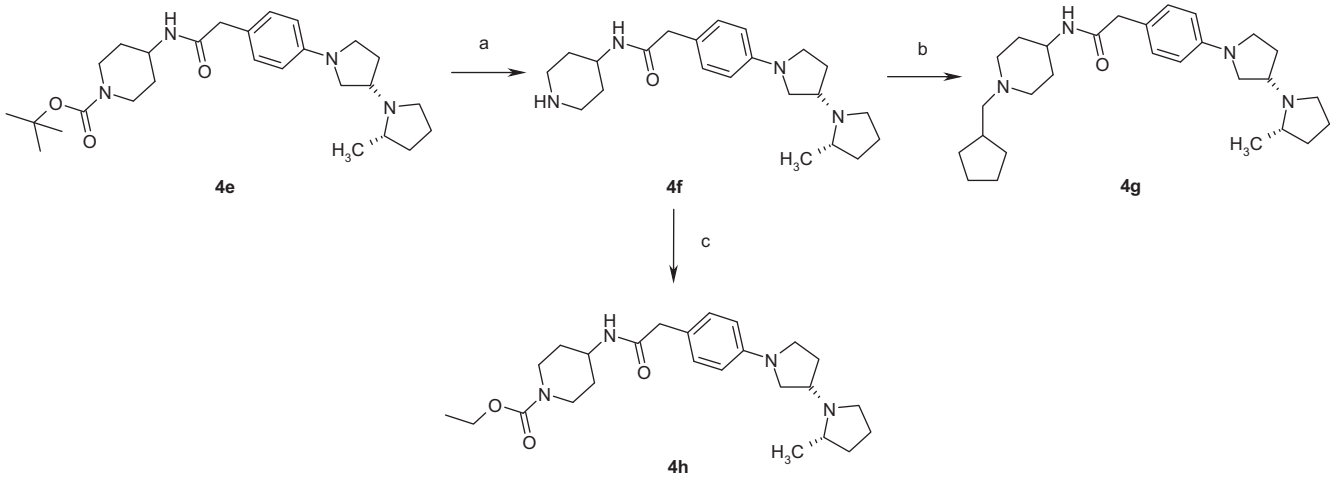

Scheme 2. Syntheses of analogs **4f**–**4h**. Reagents and conditions: (a) 4 N HCl in dioxane, thiophene, rt, overnight, 100% yield; (b) sodium triacetoxyborohydride, cyclopentane-carboxaldehyde, DCE, rt, overnight, 56% yield; (c) ethyl chloroformate, THF/water (4:1, v/v), K_2CO_3, rt, overnight, 69% yield.

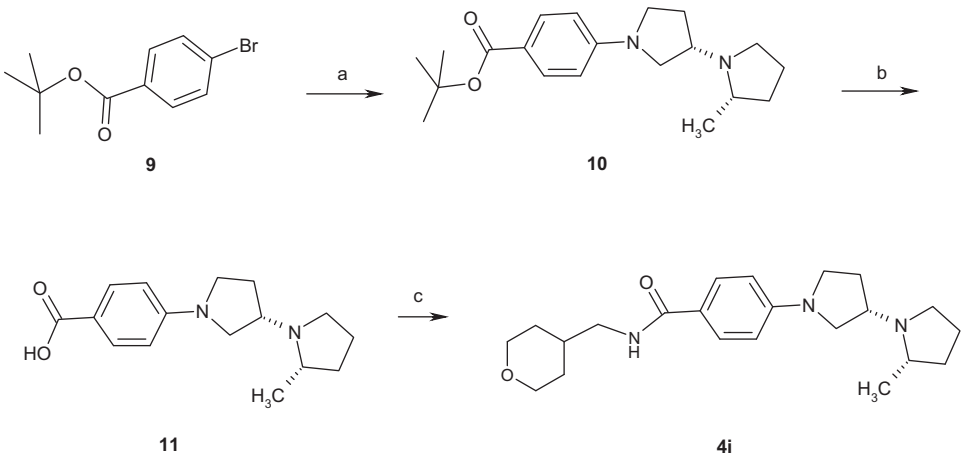

Scheme 3. Synthesis of analog **4i**. Reagents and conditions: (a) sodium *tert*-butoxide, tris(dibenzylideneacetone)-dipalladium-(0), BINAP, toluene, (2*S*,3′*S*)-2-methyl-[1,3′]bipyrrolidinyl dihydrochloride (**8**), 85 °C (external), 15 h, 60%; (b) HCl (4 M/dioxane), dioxane, rt, overnight, 100%; (c) tetrahydropyran-4-yl amine, EDC·HCl, HOBt *N*-methylmorpholine, CH_2Cl_2, DMF, rt, 16 h, 75–86% yield.

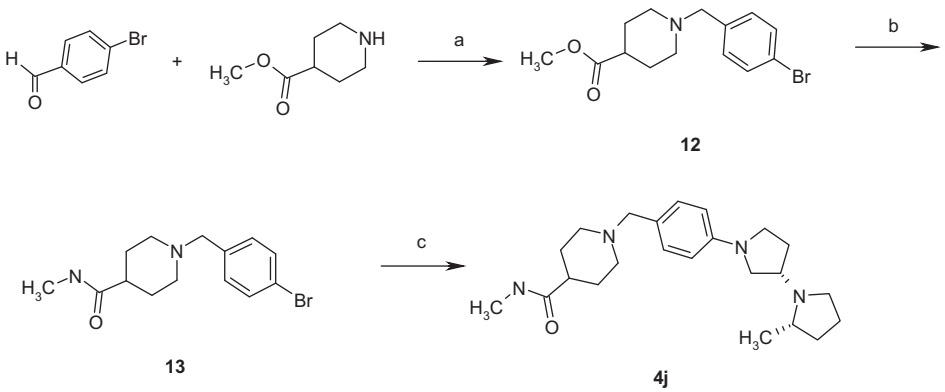

Scheme 4. Synthesis of analog **4j**. Reagents and conditions: (a) sodium triacetoxyborohydride, DCE, HCl; 92% yield; (b) $MeNH_2$, dixone, 50 °C, overnight, 46% yield; (c) sodium *tert*-butoxide, tris(dibenzylideneacetone)-dipalladium-(0), BINAP, toluene, (2*S*,3′*S*)-2-methyl-[1,3′]bipyrrolidinyl dihydrochloride (**8**), 85 °C (external), 15 h, 53%.

hERG currents is expressed as percent inhibitions at 1.0 μM and 10.0 μM concentration of the compounds tested.

The reversal of the amide's connectivity maintained H_3R affinity when compared to its close analog **2** (**4a** vs **2**). The compound also exhibited good metabolic stability and hERG channel selectivity (hERG channel percent inhibitions of 4% @ 1 μM and 20% @ 10 μM). The similar analog, **4b**, displayed very comparable results, confirming that this type of structure was worth further exploration.

As a result of these positive findings, changes to the central core were then explored. When the central core was extended by two carbons (**4c**) or one carbon (**4d**), H_3R affinity dropped slightly, but not dramatically. However, *c*log*P* increased versus **4a** and **4b**, signaling potentially better CNS penetration. Introduction of an additional basic center (**4f** and **4g** vs **4d**) restored the H_3R affinity with comparable (**4f**) or substantially increased *c*log*P* (**4g**). However, *c*log$D_{7.4}$ for **4f** was as low as −2.1, implying the possibility of a brain penetration issue. When the secondary amine was masked by a carbamate (**4h**), *c*log*P*, *c*log$D_{7.4}$, and PSA were brought within a desirable range (*c*log*P*: 1.5–2.5; *c*log$D_{7.4}$: 0.5–2.0; PSA: 45–65)[30–32] and with good H_3R affinity. Insertion of a methylene between the amine and tetrahydropyran (**4i**) maintained the rh-H_3R affinity (**4i** vs **4b**). However, the mouse H_3R affinity dropped by 4-fold, indicating the importance of distance requirements for the hydrogen bond forming elements in the mouse H_3R. Using the amine instead of the amide linker (**4j**), resulted in one of the most potent H_3R compounds. Unfortunately, the introduction of a second basic center (**4j**) resulted in lowering *c*log$D_{7.4}$ to −1.1, which is undesirable for permeability and especially for CNS penetration.[30–32] Indeed, the permeability was decreased dramatically (Caco-2/TC7 of 9.1×10^{-7} cm/s) compared to other analogs in the series.

The selected compounds (**4b**, **4c**, and **4d**) were further profiled. The physico-chemical properties were first measured and the results are presented in Table 3. Compounds **4b** and **4d** showed good solubility, while that for **4c** was much lower. Log*P* and log$D_{7.4}$ data were in a range of low, medium and high.

All three compounds were highly selective towards 33 GPCR and ion channel biological targets, with a percentage of inhibition of 30% or lower at 10 μM in the ligand binding assay. They were negative in the Ames II and in vitro micronucleus tests (MNT). Neither the three compounds displayed cytochrome P450 induction (human hepatocytes, $n = 4$; 1–60 μM for CYP1A1, CYP1A2, and CYP3A4), nor cytochrome P450 inhibition (all IC_{50} values >100 μM), indicating a low potential for drug–drug interactions. The in vitro permeability of **4b**, **4c**, and **4d** was assessed by Caco-2/TC7, with values of 111.1, 205.5, 80.8 ($\times 10^{-7}$ cm/s), respectively that predicted good intestinal absorption for all three compounds. They were stable in S9 fractions and in plasma from several species (human, guinea pig, rat, mouse, dog, monkey, sheep and rabbit) (<5% metabolized when incubated with plasmas for 4 h at 37 °C). In order to assess the hepatic metabolic liability, compounds **4c** and **4d** were incubated at 37 °C with fresh Wistar rat and CF-1 mouse liver homogenized tissues at a concentration of 5.0 μM. At the incubation time of 0, 0.33 and 2.0 hours (h), liver homogenates ($n = 3$) were analyzed with LC/MS/MS to determine the remaining percentage of parent compounds. In 2 h less than 15% of the compound was metabolized in both rat and mouse, indicating a low rate of first pass metabolism.

When the profiling data obtained thus far for these three compounds were compared side-by-side, compounds **4b** and **4d** were relatively similar while **4c** was quite different. For resources consideration, the project team decided to select only one compound from **4b** to **4d** to continue the further profiling. Thus, **4d** (from **4b** to **4d**) and **4c** were selected.

Table 2
In vitro Absorption, Distribution, Metabolism, Excretion, and Toxicity (ADMET) properties

No.	Caco-2/TC7[a]	S9 fraction liability[b] (%)			hERG inhibition[c]	
	($\times 10^{-7}$ cm/s)	Human	Mouse	Rat	% @1 μM	% @10 μM
4a	98.4	0	4	3	4	20
4b	111.1	0	6	10	14	21
4c	205.5	14	30	13	10	31
4d	80.8	0	3	13	8	19
4g	69.6	0	2	83	35	54
4h	9.6	0	0	23	32	36
4i	13.8	3	11	17	17	24
4j	9.1	ND	ND	ND	ND	ND

ND = not determined.

[a] Caco-2/TC7 (Papp, 10^{-7} cm/s) is the rate at which a compound crosses the Caco-2/TC7 monolayer under experimental conditions.

[b] S9 liability is the percent of parent compound metabolized after 15 min incubation with S9 fractions of human, mouse, and rat liver microsomes at 37 °C.

[c] hERG inhibition was determined using a patch-clamp technique in the whole-cell configuration on Chinese hamster ovary (CHO) cells. The inhibition of hERG currents is expressed as the percent inhibition at 1.0 and 10.0 μM, respectively.

Table 3
Physico-chemical properties of the selected compounds

	2	**4b**	**4c**	**4d**
Solubility (water)[a] (mg/mL)	1.1	1.13	0.004	0.60
pK_a	9.1	8.5	8.2	8.5
log*P*	1.31	2.05	3.15	1.75
log$D_{7.4}$	0.15	0.92	2.30	0.5

[a] Solubility was determined by stirring the crystalline material in pure water, quantified by HPLC.

Table 4
Pharmacokinetics of selected compounds in male CF1 mice

		4c Male CF1 mice[a]		4d Male CF1 mice[a]	
		Plasma	Brain	Plasma	Brain
iv	$AUC_{0-\infty}$ (ng·h/mL)	140	210	570	230
	$t_{1/2}$ (h)	0.19	0.13	1.0	0.75
	Cl (ng·h/mL)	14	—	3.5	—
	Vd (L/kg)	3.4	—	3.3	—
po	AUC (ng·h/mL)	240	220	1600	520
	C_{max}	403	266	1180	261
	t_{max}	0.17	0.17	0.17	1.0
	$t_{1/2}$ (h)	0.98	0.52	1.3	2.4
	F (%)	36		56	
	B/P ratio[b]	1.5		0.40	

[a] Administration at 2 mg/kg iv and 10 mg/kg po; iv formulation: 50% 1-methyl-2-pyrrolidinone in saline; concentration = 1.0 mg/mL, dosing 2 mL; po formulation: 5% DMSO/0.5% MC/0.2% Tween80, concentration = 1.0 mg/mL, dosing 10 mL.
[b] B/P ratio is 'brain to plasma' ratio calculated with iv $AUC_{0-\infty}$ exposure measured for brain and plasma tissues.

Compounds **4c** and **4d** were dosed orally to CF1 mice to measure PK parameters. The results are in Table 4. Both **4c** and **4d** displayed low plasma clearance, desirable half-life (**4c**: $t_{1/2}$ = 0.98 h; **4d** $t_{1/2}$ = 1.3 h, po), and acceptable exposure (**4c**: 240 ng·h/mL (AUC); **4d**: 1600 ng·h/mL (AUC), for a 10 mg/kg, po) with good oral bioavailability (36% and 56% for **4c** and **4d**, respectively) (Table 4). The brain AUC (ng·h/mL) values in mice were 220 and 520, respectively, when dosed orally at 10 mg/kg. The corresponding brain to plasma ratios were 0.90 and 0.35 for **4c** and **4d**, respectively.

The cardiac safety of the selected compounds **4c** and **4d** was assessed next. In order to identify compounds that not only display a low affinity towards the hERG channel, but also do not interfere with other cardiac ion channels,[33] we evaluated the effects of the selected compounds on action potentials recorded from ventricular myocytes which were isolated from guinea pigs using a method modified from that described by Salata.[34] The percent changes from the baseline (0 μM of the compound) of the action potential parameters are presented in Table 5. In this model system, **4c** did not alter the major parameters at ⩽10 μM. However, at 30 μM, the compound prolonged the action potential duration at 50% repolarization (APD_{50}) by 9% and action potential duration at 90% repolarization (ADP_{90}) by 17%, likely due to the inhibition of IKr currents. Compound **4d** shortened APD_{50} and APD_{90} at 10 μM and 30 μM, respectively. Therefore, compound **4d** was deprioritized.

Table 5
Electrophysiological effects on single ventricular myocytes isolated from guinea pigs

Parameters*	Compound	4c	4d
	Concentration (μM)	% change from baseline (0 μM)	
RMP (mV)	Control	0.0	0.0
	1	0.1 ± 0.2	0.1 ± 0.4
	3	0.2 ± 0.2	−0.2 ± 0.6
	10	0.6 ± 0.4	−0.5 ± 0.6
	30	0.0 ± 0.7	−1.1 ± 0.3
APA (mV)	Control	0.0	0.0
	1	0.1 ± 0.1	−0.5 ± 0.4
	3	0.2 ± 0.3	−1.0 ± 0.4
	10	−0.1 ± 0.4	−1.5 ± 0.5
	30	−1.0 ± 0.5	−2.4 ± 0.7
APD_{50} (ms)	Control	0.0	0.0
	1	0.0 ± 1.0	−2.3 ± 0.7
	3	2.7 ± 1.3	−5.5 ± 1.6
	10	5.9 ± 1.7	−10.3 ± 2.1
	30	9.3 ± 2.0	−17.5 ± 2.9
APD_{90} (ms)	Control	0.0	0.0
	1	0.4 ± 0.8	−1.9 ± 0.5
	3	3.4 ± 0.9	−4.2 ± 0.9
	10	8.4 ± 1.3	−7.8 ± 1.2
	30	16.9 ± 2.5	−12.3 ± 1.4

* AP, action potential; RMP, resting membrane potential; APA, action potential amplitude; APD_{50}, action potential duration at 50% of repolarization; APD_{90}, action potential duration at 90% of repolarization.

Table 6
Heart concentrations of compound **4c** after intravenous administration in anaesthetized dogs

Dose (mg/kg)	Heart sample	Tissue concentration*	
		ng/g	μM
3	Right and left ventricles	7760 ± 2250	19.0
10	Right and left ventricles	21300 ± 1550	52.3

* Limit of quantification: 15 ng/g; values are mean ± SD (n = 3).

Compound **4c** was further assessed in cardiac safety in mongrel dogs. Compound **4c**, intravenously administered at the 3 mg/kg dose to anaesthetized mongrel dogs, did not induce any major haemodynamic effect. At 10 mg/kg, iv dosing, the compound slightly decreased arterial blood pressure and heart rate but prolonged QT interval measured either under cardiac pacing or corrected for heart rate, and lengthened both auricular and ventricular refractory. This observation is consistent with the results observed by using isolated guinea pigs ventricular myocytes model system discussed above.

The cardiac tissue exposure of **4c** is listed in Table 6. Compound **4c** displayed sufficiently high cardiac exposure.

Compound **4c** was bound to plasma proteins by 51.1–66.8% and was homogeneously distributed between plasma and erythrocytes. When compared to lead **2**, which had plasma protein binding of only 30–37%, compound **4c** showed an improvement in this aspect, where protein binding almost doubled.

3. Conclusion

In summary, we have discovered a novel series of H_3R antagonists through a scaffold hopping strategy. Further SAR studies of the series culminated in the identification of ((2*S*,3′*S*)-2-methyl-[1,3′]bipyrrolidinyl-1′-yl)-naphthalene-2-carboxylic acid (tetrahydro-pyran-4-yl)-amide (**4c**) and -[4-((2*S*,3′*S*)-2-methyl-[1,3′]bipyrrolidinyl-1′-yl)-phenyl]-*N*-(tetrahydro-pyran-4-yl)-acetamide (**4d**), which exhibited good potency in H_3R binding assays, excellent selectivity, and desirable PK properties. Compounds **4c** and **4d** were also assessed in cardiac safety studies. In particular, the effects of the compounds on action potentials recorded from ventricular myocytes isolated from guinea pigs were used to screen compounds that not only displayed a low affinity towards the hERG channel, but also had lower interference with other cardiac ion channels. Both **4c** and **4d** exhibited low affinity for hERG channel, only **4c** did not alter the major parameters (APD_{50} and APD) at ⩽10 μM in this model system. Compound **4c** did not induce any major haemodynamic effect when intravenously administered at the 3 mg/kg dose to anaesthetized mongrel dogs. Compound **4c** is a new promising lead as potent H_3R antagonist with desirable PK properties belonging to a distinct structural class.

4. Experimental

4.1. Chemistry

4.1.1. General

All solvents and reagents were obtained from commercial suppliers and used without further purification unless otherwise

stated. All reactions involving dry solvents or air-sensitive agents were performed under a nitrogen atmosphere with glassware dried prior to use. Solvents were dried according to standard procedures. Reactions were monitored by analytical thin-layer chromatography (TLC) analysis and analytical High Pressure Liquid Chromatography–Mass Spectrometry (LCMS). TLC analyses are performed with EM Science silica gel 60 F_{254} plates with visualization by UV irradiation. The compounds were detected as single spots on TLC plates and visualized using UV light (254 nm) or with different spraying reagents such as $KMnO_4$, ninhydrin, and bromocresol green, respectively. Flash chromatography is performed using Alltech pre-packed silica gel cartridges on Analogix Flash chromatographic system (automatic sample collection). Eluent systems are given in volume/volume concentrations. ^{1}H NMR spectra were run at 300 MHz on a Varian Mercury 300 spectrometer with an ASW 5 mm probe, and usually recorded at ambient temperature in a deuterated solvent, such as D_2O, DMSO-d_6 or $CDCl_3$ unless otherwise noted. Chemical shifts values (δ) are indicated in parts per million (ppm) with reference to tetramethylsilane (TMS) as the internal standard and coupling constants (J) are given in Hertz (Hz). The following abbreviations are used: br = broad, s = singlet, d = doublet, dd = doublet of doublet, t = triplet, dt = doublet of triplet, tt = triplet of triplet, q = quartet, dq = doublet of quartet, m = multiplet.

LCMS experiments to determine retention times (RT) and associated mass ions are performed using one of the following methods: Mass Spectra (MS) are recorded using a Micromass mass spectrometer. Generally, the method used was positive electrospray ionization, scanning mass m/z from 100 to 1000. Liquid chromatography was performed on a Hewlett Packard 1100 Series Binary Pump & Degasser; Auxiliary detectors used were: Hewlett Packard 1100 Series UV detector, wavelength = 220 nm and Sedere SEDEX 75 Evaporative Light Scattering (ELS) detector temperature = 46 °C, N_2 pressure = 4 bar. LCT: Grad (Acetonitrile+0.05% TFA)/(H_2O+0.05% TFA) = 5:95 (0 min) to 95:5 (2.5 min) to 95:5 (3 min). Column: YMC Jsphere 33 × 24 μM, 1 ml/min.

4.1.2. 2-Methyl-4-((2*S*,3′*S*)-2-methyl-[1,3′]bipyrrolidinyl-1′-yl)-*N*-(tetrahydro-pyran-4-yl)-benzamide (4a)

Step 1. Synthesis of 4-bromo-2-methyl-*N*-(tetrahydro-pyran-4-yl)-benzamide.

4-Bromo-2-methylbenzoic acid (5.38 g, 25 mmol) was dissolved in DCM (100 mL) and DMF (25 mL) and the solution was cooled to an ice-water bath. To this solution was added a solution of tetrahydropyran-4-yl amine (2.60 g, 25 mmol, 1.0 equiv) in 10 mL of DCM, followed by *N*-methylmorpholine (5.75 g, 8 mL, 75 mmol, 3.0 equiv), 1-hydroxylbenzotriazole (HOBt) (4.40 g, 32.5 mmol, 1.3 equiv), sequentially, and finally EDC·HCl (6.25 g, 32.5 mmol, 1.3 equiv). The resultant clear light brown solution was stirred at rt overnight. TLC (10% MeOH in DCM) and LCMS detected a product peak with m/z of 299 (M+H$^+$). The reaction was quenched with saturated sodium bicarbonate aqueous solution (10 mL) and DCM (10 mL). The two layers were separated, and the aqueous layer was extracted with DCM (15 mL × 2). The combined DCM extracts were washed with sodium bicarbonate aqueous solution (10 mL) and brine (10 mL), and dried (anhydrous potassium carbonate), filtered, and concentrated in vacuo to get 6.87 g (yield 92%) of the title compound as a white solid, LCMS: RT = 2.60 min, MS: 299 (M+H$^+$). ^{1}H NMR (300 MHz, $CDCl_3$) δ 7.31 (m, 3H), 5.60 (br s, 1H), 4.10 (m, 1H), 4.01 (m, 2H), 3.53 (dt, J = 11.8, 2.1 Hz, 2H), 2.42 (s, 3H), 2.00 (m, 2H), 1.55 (m, 2H).

Step 2. Synthesis of 2-methyl-4-((2*S*,3′*S*)-2-methyl-[1,3′]bipyrrolidinyl-1′-yl)-*N*-(tetrahydro-pyran-4-yl)-benzamide.

(2*S*,3′*S*)-2-Methyl-[1,3′]bipyrrolidinyl dihydrochloride (**8**) (2.06 g, 7.83 mmol, 1.1 equiv), was dissolved in DCM (60 mL) and methanol (5 mL) with the aid of sonication. 1.14 g of powder KOH was added and the suspension was stirred at rt for 1 h. The suspension was filtrated and rinsed with DCM. The filtrate was concentrated and re-dissolved in 60 mL of anhydrous toluene.

A 200 mL of round bottomed flask was charged with 4-bromo-2-methyl-*N*-(tetrahydro-pyran-4-yl)-benzamide (2.12 g, 7.10 mmol, 1.0 equiv), sodium *tert*-butoxide (0.99 g, 10.30 mmol, 1.45 equiv), tris(dibenzylideneacetone)-dipalladium-(0) (64 mg, 0.07 mmol, 0.01 equiv), and BINAP (131 mg, 0.21 mmol, 0.03 equiv). To this flask was transferred, under nitrogen, a solution of (2*S*,3′*S*)-2-methyl-[1,3′]bipyrrolidinyl (**8**) in 60 mL of toluene prepared above. The flask was heated to 85 °C (external) with stirring until the starting material was completely consumed as judged by TLC analysis (4 h). The mixture was cooled to room temperature, diluted with ethyl acetate (20 mL) and saturated aq sodium bicarbonate (15 mL). The two layers were separated. The aqueous layer was extracted with EtOAc (3 × 15 mL). The combined organic extracts were washed with brine and dried (K_2CO_3), filtered, and concentrated. The crude product was then purified by flash chromatography on 50-g silica gel column, eluted with 0–2.5% of MeOH containing 7 N of NH_3 in DCM to obtain 2.39 g (91% yield) of a tan colored solid. Re-crystallization from methyl *t*-butyl ether (MTBE) and DCM yielded a colorless crystalline material, mp 147 °C. LCMS: RT = 1.41 min, MS: 372 (M+H$^+$). ^{1}H NMR (300 MHz, $CDCl_3$) δ 7.30 (m, 2H), 6.33 (m, 1H), 5.81 (d, J = 7.8 Hz, 1H), 4.20 (m, 1H), 3.99 (m, 2H), 3.66–3.20 (m, 7H), 3.02 (m, 1H), 2.79 (m, 1H), 2.54 (q, J = 8.4 Hz, 1H), 2.46 (s, 3H), 2.22–1.43 (m, 10H), 1.14 (d, J = 6.3 Hz, 3H).

4.1.3. 4-((2*S*,3′*S*)-2-Methyl-[1,3′]bipyrrolidinyl-1′-yl)-*N*-(tetrahydro-pyran-4-yl)-benzamide (4b)

Step 1. Synthesis of 4-bromo-*N*-(tetrahydro-pyran-4-yl)-benzamide.

Following the above procedure for **4a** step 1, 4-bromo-*N*-(tetrahydro-pyran-4-yl)-benzamide was prepared in an identical manner by coupling of tetrahydropyran-4-yl amine (0.23 g, 2.3 mmol, 1.0 equiv) with 4-bromobenzoic acid (0.51 g, 2.5 mmol, 1.1 equiv) to give 0.65 g (100% yield) as white solid. LCMS: RT = 2.57 min, MS: 285 (M+H$^+$).

Step 2. Synthesis of 4-((2*S*,3′*S*)-2-methyl-[1,3′]bipyrrolidinyl-1′-yl)-*N*-(tetrahydro-pyran-4-yl)-benzamide.

Following the above procedure for **4a**, step 2, the title compound was prepared in an identical manner by condensing (2*S*,3′*S*)-2-methyl-[1,3′]bipyrrolidinyl dihydrochloride (**8**) (0.7 g, 3.1 mmol, 1.1 equiv) with 4-bromo-*N*-(tetrahydro-pyran-4-yl)-benzamide (0.80 g, 2.8 mmol), to give 1.0 g (67% yield) as a solid. Re-crystallization from MTBE and DCM yielded a colorless crystalline material, mp 180 °C. Elemental analysis: Theoretical: C 70.55; H 8.74; N 11.75; Found: C 70.30 H 8.90 N 11.63. LC/MS: RT = 1.35 min, MS: 358 (M+H$^+$). ^{1}H NMR (300 MHz, $CDCl_3$) δ 7.62 (d, J = 8.7 Hz, 2H), 6.50 (d, J = 8.7 Hz, 2H), 5.81 (d, J = 7.8 Hz, 1H), 4.20 (m, 1H), 3.99 (m, 2H), 3.66–3.20 (m, 7H), 3.02 (m, 1H), 2.79 (m, 1H), 2.54 (q, J = 8.4 Hz, 1H), 2.22–1.43 (m, 10H), 1.14 (d, J = 6.3 Hz, 3H).

4.1.4. 6-((2*S*,3′*S*)-2-Methyl-[1,3′]bipyrrolidinyl-1′-yl)-naphthalene-2-carboxylic acid (tetrahydro-pyran-4-yl)-amide (4c)

Step 1. Synthesis of 6-bromo-naphthalene-2-carboxylic acid (tetrahydro-pyran-4-yl)-amide.

Following the above procedure for **4a**, step 1, 6-bromo-naphthalene-2-carboxylic acid (tetrahydro-pyran-4-yl)-amide was synthesized in an identical manner by coupling of tetrahydropyran-4-yl amine (0.26 g, 2.5 mmol, 1.0 equiv) with 6-bromo-naphthalene-2-carboxylic acid (0.63 g, 2.5 mmol, 1.0 equiv) to give 0.85 g (100% yield) of the title compound as a white solid. TLC (5% MeOH in DCM) R_f = 0.7. LCMS: RT = 2.85 min, MS: 335 (M+H$^+$). ^{1}H NMR (300 MHz, $CDCl_3$) δ 8.24 (s, 1H), 8.04 (s, 1H), 7.82 (m, 3H), 7.62

(m, 1H), 6.13 (m, 1H), 4.03 (m, 2H), 3.56 (dt, *J* = 2.2, 11.7 Hz, 2H), 2.06 (m, 2H), 1.62 (m, 1H).

Step 2. Synthesis of 6-((2*S*,3′*S*)-2-methyl-[1,3′]bipyrrolidinyl-1′-yl)-naphthalene-2-carboxylic acid (tetrahydro-pyran-4-yl)-amide.

Following the above procedure for **4a**, step 2, the title compound was prepared in an identical manner by condensing (2*S*,3′*S*)-2-methyl-[1,3′]bipyrrolidinyl dihydrochloride (**8**) (0.6 g, 1.1 mmol), with 6-bromo-naphthalene-2-carboxylic acid (tetrahydro-pyran-4-yl)-amide (0.57 g, 1.91 mmol), to give (64% yield) of the title compound as a fine powder. RT = 1.88 min, MS: 408 ($M+H^+$). ^1H NMR (300 MHz, $CDCl_3$) δ 8.12 (s, 1H), 7.78–7.64 (m, 3H), 7.02 (m, 1H), 6.72 (m, 1H), 6.07 (m, 1H), 4.30 (m, 1H), 4.04 (m, 2H), 3.60–3.34 (m, 7H), 3.05 (m, 1H), 2.83 (m, 1H), 2.58 (m, 1H), 2.2–1.41 (m, 10H), 1.16 (d, *J* = 6.2 Hz, 3H).

4.1.5. 2-[4-((2*S*,3′*S*)-2-Methyl-[1,3′]bipyrrolidinyl-1′-yl)-phenyl]-*N*-(tetrahydro-pyran-4-yl)-acetamide (4d)

Step 1. Synthesis of 2-(4-bromo-phenyl)-*N*-(tetrahydro-pyran-4-yl)-acetamide.

The title compound was prepared in substantially the same way as **4a**, step 1, by coupling of tetrahydropyran-4-yl amine with (4-bromo-phenyl)-acetic acid to give 0.65 g (100% yield) of the title compound as a thick oil which solidified on standing. TLC (5% MeOH in DCM) R_f = 0.6. RT = 2.57 min, MS: 299 ($M+H^+$). ^1H NMR (300 MHz, $CDCl_3$) δ 7.49 (d, *J* = 6.0 Hz, 2H), 7.13 (d, *J* = 6.0 Hz, 2H), 5.24 (br s, 1H), 3.99 (m, 3H), 3.49 (s, 2H), 3.48 (m, 2H), 1.85 (m, 2H), 1.38 (m, 2H).

Step 2. Synthesis of 2-[4-((2*S*,3′*S*)-2-methyl-[1,3′]bipyrrolidinyl-1′-yl)-phenyl]-*N*-(tetrahydro-pyran-4-yl)-acetamide.

Following the above procedure for **4a**, step 2, the title compound was prepared in an identical manner by condensing (2*S*,3′*S*)-2-methyl-[1,3′]bipyrrolidinyl dihydrochloride (**8**) (0.6 g, 1.1 mmol), with 2-(4-bromo-phenyl)-*N*-(tetrahydro-pyran-4-yl)-acetamide (0.57 g, 1.91 mmol), to give 510 mg (72% yield) of the title compound as a white solid. This was recrystallized from DCM (1 mL) and MTBE (15 mL) to get 460 mg of the title compound as a colorless crystalline material. Elemental analysis: Theoretical: C 71.12 H 8.95 N 11.31 O 8.61; Found: C 71.26 H 8.95 N 11.37 (KARL FISCHER = 0.22). Mp 155–157 °C. RT = 2.23 min, MS: 372 ($M+H^+$). ^1H NMR (300 MHz, $CDCl_3$) δ 7.08 (d, *J* = 8.4 Hz, 2H), 6.54 (d, *J* = 8.4 Hz, 2H), 5.3 (br s, 1H), 3.96 (m, 1H), 3.85 (m, 2H), 3.45 (m, 6H), 3.26 (m, 3H), 3.02 (m, 1H), 2.78 (m, 1H), 2.55 (q, *J* = 8.7 Hz, 1H), 2.21–1.71 (m, 7H), 1.48 (m, 1H), 1.31 (m, 2H), 1.14 (d, *J* = 6.6 Hz, 3H).

4.1.6. Synthesis of 2-[4-((2*S*,3′*S*)-2-methyl-[1,3′]bipyrrolidinyl-1′-yl)-phenyl]-acetylamino]-1,2-piperidine-1-carboxylic acid *tert*-butyl ester (4e)

Step 1. Synthesis of 4-[2-(4-bromo-phenyl)-acetylamino]-piperidine-1-carboxylic acid *tert*-butyl ester.

The title compound was prepared in substantially the same way as **4a**, step 1, by coupling of (4-bromo-phenyl)-acetic acid (2.84 g, 13.2 mmol, 1.1 equiv) with 4-amino-piperidine-1-carboxylic acid *tert*-butyl ester (2.4 g, 12 mmol, 1.0 equiv) to give 4.62 g (96.9% yield) of the title compound as a very white crystalline material. RT = 3.01 min, MS: 398 ($M+H^+$). ^1H NMR (300 MHz, $CDCl_3$) δ 7.49 (d, *J* = 8.4 Hz, 2H), 7.15 (d, *J* = 8.4 Hz, 2H), 5.20 (m, 1H), 3.94 (m, 3H), 3.49 (s, 2H), 2.83 (br t, *J* = 12.6, 2H), 1.85 (m, 2H), 1.44 (s, 9H), 1.20 (m, 2H).

Step 2. Synthesis of 2-[4-((2*S*,3′*S*)-2-methyl-[1,3′]bipyrrolidinyl-1′-yl)-phenyl]-acetylamino]-1,2-piperidine-1-carboxylic acid *tert*-butyl ester (**4e**).

Following the above procedure for **4a**, step 2, the title compound was prepared in an identical manner by condensing (2*S*,3′*S*)-2-methyl-[1,3′]bipyrrolidinyl dihydrochloride (**8**) (2.1 g, 7.83 mmol, 1.1 equiv), with 4-[2-(4-bromo-phenyl)-acetylamino]-piperidine-1-carboxylic acid *tert*-butyl ester (2.82 g, 7.1 mmol, 1.0 equiv), to give 3.14 g (94% yield) of the title compound as a tan colored crystalline solid. RT = 2.20 min, MS: 471 ($M+H^+$). ^1H NMR (300 MHz, $CDCl_3$) δ 7.07 (d, *J* = 8.4 Hz, 2H), 6.53 (d, *J* = 8.4 Hz, 2H), 5.26 (m, 1H), 3.91 (m, 3H), 3.56–3.35 (m, 7H), 3.02 (m, 1H), 2.81 (m, 3H), 2.53 (q, *J* = 8.4 Hz, 1H), 2.1 (m, 3H), 1.81 (m, 4H), 1.53–1.43 (m, 10H), 1.3–1.06 (m, 5H).

4.1.7. Synthesis of 2-[4-((2*S*,3′*S*)-2-methyl-[1,3′]bipyrrolidinyl-1′-yl)-phenyl]-*N*-piperidin-4-yl-acetamide (4f)

4-[2-[4-((2*S*,3′*S*)-2-Methyl-[1,3′]bipyrrolidinyl-1′-yl)-phenyl]-acetylamino]-piperidine-1-carboxylic acid *tert*-butyl ester (**4e**) (2.92 g, 6.2 mmol) was dissolved in 5 mL of dioxane. To this solution was added 1.0 g of PhSH, followed by addition of 4 N HCl in dioxane (6.2 mL, 24.8 mmol, 4 equiv). The solution was stirred at rt overnight. HCl was removed by passing nitrogen gas through the solution and the gaseous HCl was captured by a drying tube filled with NaOH.pallets. The solvent was removed by reduced pressure distillation. The residue was further dried under high vacuum to get 2.70 g (100%) of the title compound as a hydrochloride salt. LCMS: RT = 2.11 min, MS: 371 ($M+H^+$). ^1H NMR (300 MHz, $CDCl_3$) δ 11.20 (br s, 1H), 9.00 (br s, 1H), 8.21 (m, 1H), 7.12 (d, *J* = 8.7 Hz, 2H), 6.57 (d, *J* = 8.7 Hz, 2H), 3.8–3.38 (m, 7H), 3.21 (m, 3H), 2.91 (m, 3H), 2.42–2.13 (m, 5H), 1.99–1.55 (m, 8H), 1.46 (d, *J* = 6.6 Hz, 3H).

4.1.8. *N*-(1-Cyclopentylmethyl-piperidin-4-yl)-2-[4-((2*S*,3′*S*)-2-methyl-[1,3′]bipyrrolidinyl-1′-yl)-phenyl]-acetamide (4g)

To a solution of cyclopentane-carboxaldehyde (138 mg, 1.4 mmol) and 2-[4-((2*S*,3′*S*)-2-methyl-[1,3′]bipyrrolidinyl-1′-yl)-phenyl]-*N*-piperidin-4-yl-acetamide hydrochloride (**4f**) (0.52 g, 1.18 mmol) in DCE (10 mL) was added powder sodium triacetoxyborohydride slowly under N_2 at rt. The yellowish milky solution was stirred at rt overnight. LCMS showed a major peak with MS of 453. The reaction was quenched with $NaHCO_3$ (aq) (15 mL). NaOH (aq) (1 N, 5 mL) was added thereafter. The two layers were separated, and the aqueous layer was extracted with DCM (10 mL × 2). The combined DCM extracts were washed with sodium bicarbonate (10 mL), and brine (5 mL × 2), dried (anhydrous potassium carbonate), filtered, and concentrated in vacuo to get 0.30 g (56%) of the title compound as a tan solid. RT = 1.34 min, MS: 453 ($M+H^+$). ^1H NMR (300 MHz, $CDCl_3$) δ 7.06 (d, *J* = 8.7 Hz, 2H), 6.52 (d, *J* = 8.7 Hz, 2H), 5.24 (m, 1H), 3.75 (m, 1H), 3.52 (m, 2H), 3.45 (s, 2H), 3.38–3.20 (m, 3H) 3.03 (m, 1H), 2.74 (m, 2H), 2.56 (d, *J* = 8.4 Hz, 1H), 2.21–1.93 (m, 8H), 1.86–1.43 (m, 14H), 1.27 (m, 2H), 1.14 (d, *J* = 6.3 Hz, 3H).

4.1.9. 4-[2-[4-((2*S*,3′*S*)-2-Methyl-[1,3′]bipyrrolidinyl-1′-yl)-phenyl]-acetylamino]-piperidine-1-carboxylic acid ethyl ester (4h)

2-[4-((2*S*,3′*S*)-2-Methyl-[1,3′]bipyrrolidinyl-1′-yl)-phenyl]-*N*-piperidin-4-yl-acetamide hydrochloride (**4f**) (0.51 g, 1.38 mmol) was dissolved in THF (20 mL) and water (5 mL) to form a clear solution. To this solution was added 0.30 g of ethyl chloroformate (3.00 mmol, 2.0 equiv), followed by K_2CO_3 (0.76 g, 5.52 mmol, 4.0 equiv). The clear solution was stirred at rt overnight. TLC (5% of 7 N NH_3/MeOH in DCM) showed the starting material was consumed completely. LCMS: a single peak with MS of 443 ($M+H^+$) was detected. The reaction was diluted with EtOAc (10 mL) and water (15 mL). The two layers were separated and the aqueous layer was extracted with EtOAc (2 × 10 mL). The combined organic solution was washed with brine (2 × 10 mL), dried (K_2CO_3), filtered, and concentrated. The crude product was purified on a 25-g silica gel column eluted with 0–5% MeOH in DCM to get 0.42 g (69%) of the title compound as a tan solid. LCMS: RT = 1.88 min, MS: 443 ($M+H^+$). ^1H NMR (300 MHz, $CDCl_3$) δ 7.06 (d, *J* = 8.7 Hz, 2H), 6.53 (d, *J* = 8.7 Hz, 2H), 5.28 (m, 1H), 4.09 (q, *J* = 7.2 Hz, 2H),

3.94–3.52 (m, 4H), 3.40 (s, 2H), 3.44–3.18 (m, 6H), 3.03 (m, 1H), 2.88 (m, 2H), 2.78 (m, 1H), 2.54 (d, J = 8.4 Hz, 1H), 2.21–1.69 (m, 8H), 1.49 (m, 1H), 1.23 (t, J = 7.2 Hz, 3H), 1.14 (d, J = 6.2 Hz, 3H).

4.1.10. 4-((2*S*,3′*S*)-2-Methyl-[1,3′]bipyrrolidinyl-1′-yl)-*N*-(tetrahydro-pyran-4-yl-methyl)-benzamide (4i)

Step 1. Synthesis of 4-((2*S*,3′*S*)-2-methyl-[1,3′]bipyrrolidinyl-1′-yl)-benzoic acid *tert*-butyl ester (**10**).

(2*S*,3′*S*)-2-Methyl-[1,3′]bipyrrolidinyl dihydrochloride (**8**) (1.1 g, 4 mmol) was treated with NaOt-Bu (1.1 g, 2equiv) in MeOH (30 mL), filtered, and concentrated. To this flask was added *tert*-butyl-4-bromo-benzoate (**9**) (1.0 g, 3.89 mmol), sodium *tert*-butoxide (538 mg, 5.6 mmol), tris(dibenzylideneacetone)-dipalladium-(0) (35 mg, 0.039 mmol), BINAP (72 mg, 0.116 mmol), and toluene (40 mL) under nitrogen. The reaction flask was heated to 80 °C (external) for 24 h with stirring until the starting material was completely consumed as judged by TLC analysis. The mixture was cooled to room temperature, taken up in DCM (50 mL), filtered, and concentrated. The crude product was then purified by a silica gel flash chromatography eluted with 0–5% of 7 N NH_3/MeOH in DCM to get 1.02 g (80%) of the title compound as a yellow oil. LCMS: RT = 2.23 min, MS: 331 ($M+H^+$). ^1H NMR (300 MHz, $CDCl_3$) δ 7.87 (d, J = 8.7 Hz, 2H), 6.49 (d, J = 8.7 Hz, 2H), 3.6–3.23 (m, 5H), 3.01 (m, 1H), 2.78 (m, 1H), 2.55 (q, J = 8.4 Hz, 1H), 2.22–1.43 (m, 13H), 1.14 (d, J = 6.3 Hz, 3H).

Step 2. Synthesis of 4-((2*S*,3′*S*)-2-methyl-[1,3′]bipyrrolidinyl-1′-yl)-benzoic acid (**11**).

4-((2*S*,3′*S*)-2-Methyl-[1,3′]bipyrrolidinyl-1′-yl)-benzoic acid *tert*-butyl ester (**10**) (0.28 g, 0.8 mmol) was treated with 5 mL of 4 N HCl in dioxane at rt overnight. The HCl was removed by passing nitrogen gas through the solution and the gaseous HCl was captured by a drying tube filled with NaOH.pallets. The solvent was evaporated to dryness and dried further under high vacuum to yield 0.37 g (HCl salt, ~100%) of the title compound as a white powder. TLC (5% MeOH in DCM) R_f = 0.6.

Step 3. Synthesis of 4-((2*S*,3′*S*)-2-methyl-[1,3′]bipyrrolidinyl-1′-yl)-*N*-(tetrahydro-pyran-4-yl-methyl)-benzamide (**4i**).

4-((2*S*,3′*S*)-2-Methyl-[1,3′]bipyrrolidinyl-1′-yl)-benzoic acid (**11**) (0.17 g, 0.625 mmol) was dissolved in DCM (4 mL) and DMF (2 mL) and the solution was cooled to an ice-water bath. To this solution was added a solution of tetrahydropyran-4-yl amine (0.10 g, 0.86 mmol, 1 equiv) in 1 mL of DCM, followed by *N*-methylmorpholine (0.2 mL, 3 equiv), 1-hydroxylbenzotriazole (HOBt) (0.11 g, 1.3 equiv), sequentially, and finally EDC·HCl (104 mg, 1.3 equiv). The resultant clear light brown solution was stirred at rt overnight. TLC (10% MeOH in DCM) and LC/MS detected the product peak at retention time of 2.15 min with MS of 372. The reaction was quenched with saturated sodium bicarbonate aqueous solution (10 mL) and 10 mL of DCM. The two layers were separated, and the aqueous layer was extracted with DCM (15 mL × 2). The combined DCM extracts were washed with sodium bicarbonate (10 mL), and brine (10 mL), dried (anhydrous potassium carbonate), filtered, and concentrated in vacuo to get 0.17 g (74%) of the titled compound as a solid. LCMS: RT = 1.43 min, MS: 372 ($M+H^+$). ^1H NMR (300 MHz, $CDCl_3$) δ 7.68 (d, J = 8.7 Hz, 2H), 6.52 (d, J = 8.7 Hz, 2H), 6.08 (s, 1H), 3.98 (m, 2H), 3.66–3.20 (m, 7H), 3.02 (m, 1H), 2.78 (m, 1H), 2.54 (q, J = 8.4 Hz, 1H), 2.22–1.43 (m, 10H), 1.54–1.30 (m, 3H), 1.14 (d, J = 6.3 Hz, 3H).

4.1.11. 1-[4-((2*S*,3′*S*)-2-Methyl-[1,3′]bipyrrolidinyl-1′-yl)-benzyl]-piperidine-4-carboxylic acid methylamide hydrochloride (4j)

Step 1. Synthesis of 1-(4-bromo-benzyl)-piperidine-4-carboxylic acid methyl ester (**12**).

To a solution of 4-bromo-benzaldehyde (3.88 g, 21 mmol, 1.05 equiv) in DCE (60 mL) was added piperidine-4-carboxylic acid methyl ester (2.86 g, 20 mmol), followed by 4 N HCl (6 mL, 24 mmol, 1.2 equiv) and powder sodium triacetoxyborohydride slowly under N_2 at rt. The yellowish milky solution was stirred at rt overnight. LCMS of the reaction mixture: RT = 2.43 min, MS = 314 (77%) with impurity at 2.72 min, MS = 425 (23%).

The reaction was quenched with aq $NaHCO_3$ solution. The two layers were separated, and the aqueous layer was extracted with DCM (10 mL × 2). The combined DCM extracts were washed with sodium bicarbonate (10 mL), and brine (5 mL × 2), dried (anhydrous potassium carbonate), filtered, and concentrated in vacuo to get 5.71 g (yield: 92%) of the ester (**12**) as a liquid.

Step 2. Synthesis of 1-(4-bromo-benzyl)-piperidine-4-carboxylic acid methyl amide (**13**).

The ester (**12**) (0.5 g, crude as such obtained above, about 1.6 mmol) was dissolved in dioxane (5 mL). To this solution was added aqueous $MeNH_2$ (40% w/w, 2.5 mL, excess). The clear colorless solution was stirred over an oil bath heating at 50 °C overnight. LCMS did not detect the SM, but a product with MS of 312, along with the impurity at 2.332 min with MS of 424.

The solvent was removed via reduced pressure distillation. The residue was taken in 5 mL of DCM and 5 mL of aq $NaHCO_3$. The two layers were separated. The aqueous layer was extracted with DCM (3 × 15 mL). The combined organic extracts were washed with brine and dried (K_2CO_3), filtered, and concentrated. The crude product was then purified by flash chromatography on 25-g silica gel column, eluted with 0–2.5% of 7 N NH_3/MeOH in DCM to obtain 0.23 g (46% yield) of the title compound (**13**) as a white powder. RT = 1.41 min, MS: 312 ($M+H^+$). ^1H NMR (300 MHz, $CDCl_3$) δ 7.44 (d, J = 8.4 Hz, 2H), 7.20 (d, J = 8.4 Hz, 2H), 5.45 (br s, 1H), 3.43 (s, 2H), 2.89 (m, 2H), 2.82 (d, J = 4.8 Hz, 3H), 2.13–1.92 (m, 3H), 1.84–1.70 (m, 4H).

Step 3. Synthesis of 1-[4-((2*S*,3′*S*)-2-methyl-[1,3′]bipyrrolidinyl-1′-yl)-benzyl]-piperidine-4-carboxylic acid methyl amide (**4j**).

A round bottomed flask (100 mL) was charged with 1-(4-bromo-benzyl)-piperidine-4-carboxylic acid methyl amide (**13**) (230 mg, 0.74 mmol, 1 equiv), sodium *tert*-butoxide (102 mg, 1.07 mmol, 1.45 equiv), tris(dibenzylideneacetone)-dipalladium-(0), and BINAP. To this flask was transferred a solution of the amine (0.25 M, pre-made from (2*S*,3′*S*)-2-methyl-[1,3′]bipyrrolidinyl dihydrochloride (**8**), 3.7 mL, 0.925 mmol, 1.2 equiv) in toluene under nitrogen. The flask was heated to 85 °C (external) with stirring until the starting material was completely consumed (6 h) as judged by TLC analysis. LC/MS: RT = 1.703 min; MS = 385.

The mixture was cooled to room temperature, diluted with ethyl acetate (20 mL) and aq sodium bicarbonate (15 mL). The two layers were separated. The aqueous layer was extracted with EtOAc (3 × 15 mL). The combined organic extracts were washed with brine and dried (K_2CO_3), filtered, and concentrated. The crude product was then purified by flash chromatography on 25-g silica gel column, eluted with 0–2.5% of 7 N NH_3/MeOH in DCM to obtain 150 mg (53% yield) of the title compound as an oil. This was dissolved in 1 mL of DCM, added 0.5 mL of 1 N HCl in ether. The white precipitate formed was collected and further dried to get 155 mg of the title compound as a HCl salt. LCMS: RT = 1.77 min, MS = 385 ($M+H^+$). ^1H NMR (300 MHz, DMSO) δ 7.89 (m, 1H), 7.44 (d, J = 8.4 Hz, 2H), 7.20 (d, J = 8.4 Hz, 2H), 4.2–3.89 (m, 3H), 3.76–3.17 (m, 5H), 3.43 (s, 2H), 2.89 (m, 2H), 2.56 (d, J = 5.1 Hz, 3H), 2.13–1.92 (m, 6H), 1.84–1.70 (m, 7H), 1.46 (d, J = 6.6 Hz, 3H).

4.2. Pharmacology

4.2.1. H_3R binding inhibition constant (K_i) determination

The H_3R radio ligand binding assay was performed using H_3 receptor membranes prepared from the Flp-In T-REx 293 Cell Line (Invitrogen) stably transfected with pcDNA5/FRT/TO (Invitrogen) containing the human or rhesus monkey (*Macaca mulatta*) or rat (*Rattus norvegicus*) 445 amino acid H_3 receptor. [^{3}H]-methylhistamine is purchased from Perkin Elmer and wheat germ agglutinin

scintillation proximity assay (WGA SPA) beads are from Amersham. The assay was performed in 96-well opti-plates (Packard). Each reaction contained 50 μl H_3R membranes (20–30 μg total protein), 50 μl WGA SPA beads (0.1 μg) and 50 μl of 83 Ci/mmol [^{3}H]-methylhistamine (final concentration 2 nM) and 50 μl of tested compound. The exemplified compounds and/or vehicle were diluted with binding buffer from 10 mM DMSO solutions. Assay plates were sealed with TopSeal (Perkin Elmer) and mixed on shaker (25 °C, 1 h). Assay plates were read on TopCount scintillation counter (Packard). Results were analyzed by Hill transformation and K_i values were determined by Cheng–Prusoff equation.

4.3. Drug safety

4.3.1. Patch-clamp recording from CHO cells

Patch-clamp technique was used to evaluate the hERG channel affinity of compounds as described previously.[35] Chinese hamster ovary (CHO) cells stably expressing the hERG cardiac potassium channels were seeded on glass coverslips 12–48 h prior to patch-clamp recording. Whole-cell configuration of the patch-clamp technique was used to record hERG currents from CHO cells on a coverslip. Electrodes were filled with pipette solution containing 120 mM potassium aspartate, 20 mM KCl, 4 mM Na_2ATP, 5 mM HEPES, 1 mM $MgCl_2$, pH 7.2 with KOH (resistance: 2–4 M Ω). The recording chamber was perfused with external solution containing 130 mM NaCl, 5 mM KCl, 2.8 mM sodium acetate, 1.0 mM $MgCl_2$, 10 mM HEPES, 10 mM glucose, 1.0 mM $CaCl_2$, pH 7.4 with NaOH. Currents were recorded at room temperature using an Axopatch 200B amplifier (Molecular Devices LLC, Sunnyvale, CA) and analyzed using the pCLAMP software (Molecular Devices LLC.).

4.3.2. Action potential recording from guinea pig myocytes

Single ventricular myocytes were isolated from guinea pigs with procedures and protocols approved by the Sanofi Institutional Animal Care and Use Committee (Bridgewater, New Jersey). Myocyte isolation, action potential recording, and data analysis were performed as described previously.[35] Briefly, male guinea pigs (Hartley) were anesthetized and a thoracotomy was performed. The heart was quickly excised and perfused retrogradely at 10 mL/min through the aorta with modified Tyrode's solution (containing 132 mM NaCl, 4 mM KCl, 1.2 mM $MgCl_2$, 10 mM HEPES, and 10 mM glucose, pH adjusted to 7.4 with 10 M NaOH) for 4 min followed by an 8-min perfusion with modified Tyrode's solution containing 102 units/ml Type 2 collagenase (271 units/mg, Worthington Biochemical Corporation, Lakewood, NJ) and 0.6 units/ml Type XIV protease (4 units/mg, Sigma Chemical Co., St. Louis, MO). The left ventricle was cut into small pieces and gently bubbled with 100% O_2 at room temperature for ~2 min to disperse single myocytes, which were maintained at room temperature for electrophysiological recording, usually within 5 h of isolation.

Ventricular myocytes in a recording chamber with the temperature set at 37 ± 1 °C were perfused with the modified Tyrode's solution containing 1.8 mM $CaCl_2$. Action potentials were initiated from a myocyte at 1 Hz current pulses using glass microelectrodes (filled with 3 M KCl, Resistance = 20–45 M Ω). Action potential signals were amplified using an Axoclamp 2B amplifier (Molecular Devices LLC.) and stored for analysis with the pCLAMP software (Molecular Devices, LLC.).

Acknowledgements

The authors greatly appreciate Sanofi R&D management for their strong support, the H_3R project team members for their contributions, the Sanofi analytical department for their support utilizing analytical studies to confirm compound structures, perform solid state characterizations, formulation support and the Sanofi DMPK and Drug Safety department for PK and in vitro/in vivo drug safety assessments.

References and notes

1. Arrang, J. M.; Garbarg, M.; Schwartz, J. C. *Nature* **1983**, *302*, 832.
2. Singh, M.; Jadhav, H. R. *Mini-Rev. Med. Chem.* **2013**, *13*, 47.
3. Berlin, M.; Boyce, C. W.; Ruiz Mde, L. *J. Med. Chem.* **2011**, *54*, 26.
4. Lazewska, D.; Kiec-Kononowicz, K. *Expert Opin. Ther. Patents* **2010**, *20*, 1147.
5. Gemkow, M. J.; Davenport, A. J.; Harich, S.; Ellenbroek, B. A.; Cesura, A.; Hallett, D. *Drug Discovery Today* **2009**, *14*, 509.
6. Esbenshade, T. A.; Browman, K. E.; Bitner, R. S.; Strakhova, M.; Cowart, M. D.; Brioni, J. D. *Br. J. Pharmacol.* **2008**, *154*, 1166.
7. Wijtmans, M.; Leurs, R.; de Esch, I. *Expert Opin. Invest. Drugs* **2007**, *16*, 967.
8. Leurs, R.; Blandina, P.; Tedford, C.; Timmerman, H. *Trends Pharmacol. Sci.* **1998**, *19*, 177.
9. Alves-Rodrigues, A.; Timmerman, H.; Willems, E.; Lemstra, S.; Zuiderveld, O. P.; Leurs, R. *Brain Res.* **1998**, *788*, 179.
10. Weisler, R. H.; Pandina, G. J.; Daly, E. J.; Cooper, K.; Gassmann-Mayer, C.; Investigators, A. T. T. S. *CNS Drugs* **2012**, *26*, 421.
11. Cowart, M.; Faghih, R.; Curtis, M. P.; Gfesser, G. A.; Bennani, Y. L.; Black, L. A.; Pan, L.; Marsh, K. C.; Sullivan, J. P.; Esbenshade, T. A.; Fox, G. B.; Hancock, A. A. *J. Med. Chem.* **2005**, *48*, 38.
12. Vohora, D.; Bhowmik, M. *Front. Syst. Neurosci.* **2012**, *6*, 72.
13. Herring, W. J.; Wilens, T. E.; Adler, L. A.; Baranak, C.; Liu, K.; Snavely, D. B.; Lines, C. R.; Michelson, D. *J. Clin. Psychiatry* **2012**, *73*, e891.
14. Haig, G. M.; Bain, E.; Robieson, W.; Othman, A. A.; Baker, J.; Lenz, R. A. *Schizophr. Bull.* **2014**, *40*, 1433.
15. Esbenshade, T. A.; Fox, G. B.; Cowart, M. D. *Mol. Interventions* **2006**, *6*, 77.
16. Hancock, A. A.; Diehl, M. S.; Fey, T. A.; Bush, E. N.; Faghih, R.; Miller, T. R.; Krueger, K. M.; Pratt, J. K.; Cowart, M. D.; Dickinson, R. W.; Shapiro, R.; Knourek-Segel, V. E.; Droz, B. A.; McDowell, C. A.; Krishna, G.; Brune, M. E.; Esbenshade, T. A.; Jacobson, P. B. *Inflamm. Res. Official J. Eur. Histamine Res. Soc.* **2005**, *54*, S27.
17. Bhowmik, M.; Khanam, R.; Vohora, D. *Br. J. Pharmacol.* **2012**, *167*, 1398.
18. McGaraughty, S.; Chu, K. L.; Cowart, M. D.; Brioni, J. D. *J. Pharmacol. Exp. Ther.* **2012**, *343*, 13.
19. Levi, R.; Seyedi, N.; Schaefer, U.; Estephan, R.; Mackins, C. J.; Tyler, E.; Silver, R. B. *Biochem. Pharmacol.* **2007**, *73*, 1146.
20. Kuhne, S.; Wijtmans, M.; Lim, H. D.; Leurs, R.; de Esch, I. J. *Expert Opin. Invest. Drugs* **2011**, *20*, 1629.
21. Celanire, S.; Wijtmans, M.; Talaga, P.; Leurs, R.; de Esch, I. J. *Drug Discovery Today* **2005**, *10*, 1613.
22. Schwartz, J. C. *Br. J. Pharmacol.* **2011**, *163*, 713.
23. Gao, Z.; Hurst, W. J.; Czechtizky, W.; Hall, D.; Moindrot, N.; Nagorny, R.; Pichat, P.; Stefany, D.; Hendrix, J. A.; George, P. G. *Bioorg. Med. Chem. Lett.* **2013**, *23*, 6269.
24. Gao, Z.; Hurst, W. J.; Guillot, E.; Czechtizky, W.; Lukasczyk, U.; Nagorny, R.; Pruniaux, M. P.; Schwink, L.; Sanchez, J. A.; Stengelin, S.; Tang, L.; Winkler, I.; Hendrix, J. A.; George, P. G. *Bioorg. Med. Chem. Lett.* **2013**, *23*, 3421.
25. Gao, Z.; Hurst, W. J.; Guillot, E.; Czechtizky, W.; Lukasczyk, U.; Nagorny, R.; Pruniaux, M. P.; Schwink, L.; Sanchez, J. A.; Stengelin, S.; Tang, L.; Winkler, I.; Hendrix, J. A.; George, P. G. *Bioorg. Med. Chem. Lett.* **2013**, *23*, 3416.
26. Gao, Z.; Hurst, W. J.; Czechtizky, W.; Francon, D.; Griebel, G.; Nagorny, R.; Pichat, P.; Schwink, L.; Stengelin, S.; Hendrix, J. A.; George, P. G. *Bioorg. Med. Chem. Lett.* **2013**, *23*, 6141.
27. Gao, Z.; Hurst, W. J.; Guillot, E.; Nagorny, R.; Pruniaux, M. P.; Hendrix, J. A.; George, P. G. *Bioorg. Med. Chem. Lett.* **2013**, *23*, 4044.
28. Wolfe, J. P.; Buchwald, S. L. *J. Org. Chem.* **2000**, *65*, 1144.
29. Wolfe, J. P.; Tomori, H.; Sadighi, J. P.; Yin, J.; Buchwald, S. L. *J. Org. Chem.* **2000**, *65*, 1158.
30. Vilar, S.; Chakrabarti, M.; Costanzi, S. *J. Mol. Graphics Modell.* **2010**, *28*, 899.
31. Summerfield, S. G.; Read, K.; Begley, D. J.; Obradovic, T.; Hidalgo, I. J.; Coggon, S.; Lewis, A. V.; Porter, R. A.; Jeffrey, P. *J. Pharmacol. Exp. Ther.* **2007**, *322*, 205.
32. Ravula, S. B.; Yu, J.; Tran, J. A.; Arellano, M.; Tucci, F. C.; Moree, W. J.; Li, B. F.; Petroski, R. E.; Wen, J.; Malany, S.; Hoare, S. R.; Madan, A.; Crowe, P. D.; Beaton, G. *Bioorg. Med. Chem. Lett.* **2012**, *22*, 421.
33. Roden, D. M.; Balser, J. R.; George, A. L., Jr.; Anderson, M. E. *Annu. Rev. Physiol.* **2002**, *64*, 431.
34. Salata, J. J.; Wasserstrom, J. A. *Circ. Res.* **1988**, *62*, 324.
35. Kang, J.; Chen, X. L.; Wang, H.; Ji, J.; Cheng, H.; Incardona, J.; Reynolds, W.; Viviani, F.; Tabart, M.; Rampe, D. *Mol. Pharmacol.* **2005**, *67*, 827.